Solar Energy Materials and Solar Cells 185 (2018) 260–269

Contents lists available at ScienceDirect

Solar Energy Materials and Solar Cells

journal homepage: www.elsevier.com/locate/solmat

SiO_2 surface passivation layers – a key technology for silicon solar cells

Stefan W. Glunz[a,b,*], Frank Feldmann[a,b]

[a] Fraunhofer Institute for Solar Energy Systems, Heidenhofstrasse 2, D-79110 Freiburg, Germany
[b] Laboratory for Photovoltaic Energy Conversion, Department of Sustainable Systems Engineering, Albert-Ludwigs-University Freiburg, Germany

ABSTRACT

High-efficiency silicon solar cells strongly rely on an effective reduction of charge carrier recombination at their surfaces, i.e. surface passivation. Today's industrial silicon solar cells often utilize dielectric surface passivation layers such as SiN_x and Al_2O_3. However, a passivation layer well-known from the microelectronic industry, SiO_2, had and has a strong impact on silicon photovoltaics. It allowed to develop the first 20% efficient silicon solar cells in the past and currently experiences a renaissance as the interfacial oxide for silicon-based passivating contacts, thus enabling the next generation of silicon solar cells. This article reviews the properties of SiO_2 passivation layers and their strong impact on the historical and current development of silicon solar cells.

1. Surface passivation of silicon solar cells

1.1. Recombination losses

Photovoltaic energy conversion based on crystalline silicon solar cells is one of the major technological pillars for the enormous success of renewable energies in the last decade. The rapid reduction of levelized costs of electricity is achieved by reduced production costs and increased conversion efficiencies. The ways to increase conversion efficiency are manifold. This task can be compared with fixing a leaky bucket [1,2] which is used to collect as much water as possible. Since the bucket has many holes the question arises which is the first one to be fixed to obtain a better “water collection efficiency”, i.e. cell efficiency.

The holes symbolize different losses as resistive and optical losses and recombination of photo-generated charge carriers. The latter one is often regarded as the most detrimental and complex loss channel in a solar cell. We can distinguish between extrinsic recombination as (Fig. 1)

- surface defect recombination and
- Shockley-Read-Hall recombination via bulk defects

and intrinsic recombination as

- Auger and
- radiative recombination.

Indeed, the leaky bucket features a variety of different holes with different diameters. Therefore, before starting to fix the bucket, a detailed analysis of the situation should be performed. This is a challenging task since there is a strong interaction between the different recombination losses. Fig. 2 shows the intrinsic and extrinsic recombination loss currents of a silicon solar cell at maximum power point (mpp) as a function of the surface recombination at the rear side (S_{back}) [3]. If the surface recombination velocity at the rear side is high (S_{back} = 1000 cm/s), we observe a very high loss current of more than 3.5 mA/cm^2 (red area) while the other recombination channels (grey areas) seem to play a negligible role. Therefore, fixing this biggest hole in the bucket should be tackled by reducing the surface recombination velocity at the rear side. In the last decades such reduction of the surface recombination was in fact among the most important improvements of silicon solar cells. And in fact, less water is running out of the bucket, i.e. the total recombination current at mpp is significantly reduced.

While the total recombination loss is reduced with decreasing S_{back}, the loss currents of the other recombination channels are increasing not only relatively but also *absolutely* although material properties such as the bulk lifetime have not changed. The higher absolute loss results from the higher amount of available free charge carriers. In other words: Due to fixing one of the holes (“rear surface recombination”), the water level in the bucket has been raised and the leakage through the other holes is getting larger. This demonstrates the complexity of the optimization of a solar cell which is getting even more complex in real world since additional interactions in the process sequence have to be taken into account.

* Corresponding author.
E-mail address: stefan.glunz@ise.fraunhofer.de (S.W. Glunz).

https://doi.org/10.1016/j.solmat.2018.04.029
Received 22 February 2018; Received in revised form 19 April 2018; Accepted 23 April 2018

Fig. 1. The leaky bucket (Drawing: Courtesy of Willi Gertsen, 2018).

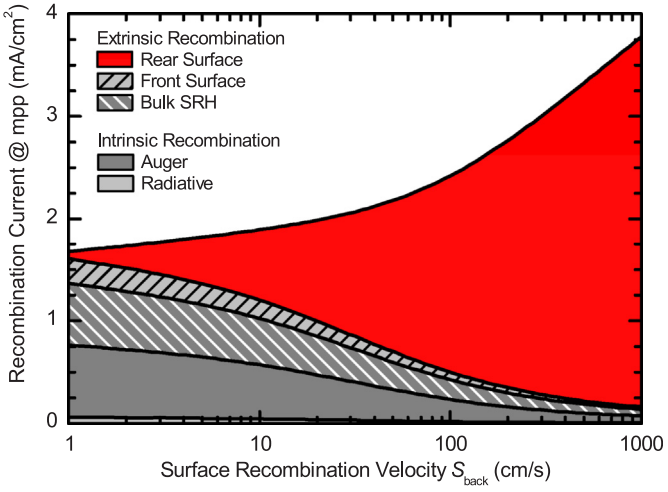

Fig. 2. Recombination losses of silicon solar cells as a function of recombination velocity at the rear side (Data taken from [3]).

1.2. Dielectric layers for surface passivation

The reduction of surface recombination at the front and rear of the solar cell was definitely one of the most important technological advances for industrial $n^+p\,p^+$ cells in the last decades [4,5]. Reducing the recombination at the front surface and thus in the emitter with SiN_x layers [6] deposited using plasma-enhanced chemical vapor deposition (PECVD) has improved the blue response and the open-circuit voltage (V_{oc}) of solar cells. The high concentration of hydrogen in such SiN_x layers is partly released in the final firing metallization step and results in an additional hydrogen passivation of bulk defects in multicrystalline silicon. Thus, we have fixed two holes with one additional cell feature. Also, the reduction of the recombination at the rear side had a strong impact since the thickness of industrial solar cells was reduced from more than 300 µm to less than 200 µm in the last decades. This diminishes the impact of bulk recombination while the recombination at the rear surface is getting more and more dominant. As a first measure to reduce S_{back}, the quality of the aluminum paste and the related firing step used for the creation of the $p\,p^+$ high-low junction (back surface field, BSF) was strongly improved. This resulted in silicon solar cells with efficiencies around 20% [7].

For an even more effective suppression of surface recombination, rear structures with partial contacts (PRC) and dielectric surface passivation are transferred into industrial production [8]. This structure well-known as passivated emitter and rear cell (PERC) has additionally the advantage to improve the internal reflection of long-wavelength light. The strong positive charge of the SiN_x layer which is used to passivate the n-type emitter of n^+-p industrial cells would result in an inversion layer on the weakly doped p-type rear surface. Therefore, a new passivation layer with a strong negative charge, Al_2O_3, was introduced to photovoltaics a few years ago [9,10]. Such layers are either deposited by atomic layer deposition or plasma-enhanced vapor deposition [11]. Most of today's PERC-type solar cells use Al_2O_3 with an additional SiN_x capping layer allowing for conversion efficiencies of around 22% and 21% on mono- and multicrystalline silicon, respectively [12,13].

However, when reviewing today´s most frequently used dielectric layers for the rear surface passivation of PERC cells in industrial production, i.e. SiN_x and Al_2O_3 [8], one should not forget the most influential and natural surface passivation for silicon solar cells: thermally grown silicon dioxide, SiO_2. In this article we will review the impact of SiO_2 surface passivation layers which have allowed for the successful development of silicon solar cells with efficiencies of more than 20%. Actually, SiO_2 experiences a renaissance as the interfacial oxide for silicon-based passivating contacts for the next generation of silicon solar cells as discussed in the second part of this publication.

2. SiO_2 for photovoltaic applications – a review

It is fair to say that the passivation of the surfaces of silicon solar cells was THE enabler for achieving efficiencies greater than 20%. The first and most natural choice for surface passivation is a thermally grown SiO_2. Thermal oxides were the key technology for microelectronics [14–16] and were adapted already very early in the history of silicon solar cells.

2.1. Metal insulator semiconductor solar cells

One of the first applications of oxides in silicon photovoltaics was as a thin intermediate layer in metal-insulator-silicon (MIS) structures [17–21]. The oxide allows to reduce the recombination at the metal interface and to utilize the work function difference between the metal contact and silicon in the semiconductor more effectively thereby inducing an effective junction. The junction between the front metal contacts could be either established by an inversion layer (IL) enhanced by charges incorporated in a SiN_x layer [21] or by an additional phosphorus diffusion resulting in the so called MIS-n^+p (MINP) cell structure [22]. Such MINP cells showed a high open-circuit voltage of 678 mV [23] and a very good blue response. The MIS-IL cell (see Fig. 3) was later produced by the German company Nukem [24].

Thin oxides were also used in polysilicon/SiO_x structures [25,26] for photovoltaic applications which have experienced a renaissance in the last years as described in detail in a later section of this paper.

2.2. Front surface passivation

In most of today´s silicon solar cells more conventional contacts are utilized where the passivation layer is only applied in-between the front contact and a direct metal-semiconductor contact is established. In 1978, Fossum and Burgess [27] oxidized the front surface of a simple $p^+\,n\,n^+$ BSF cell with a thin SiO_2 layer and achieved open-circuit voltages in the range of 620 mV compared to cells without oxide exhibiting only up to 590 mV. Later on this concept was optimized and led to the first passivated emitter solar cells (PESC) [28]. The PESC structure featured a contact opening in the front oxide smaller than the contact finger itself, reducing the metal-semiconductor recombination.

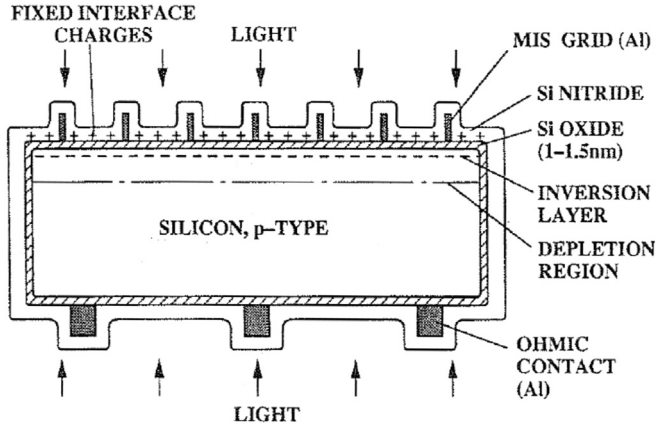

Fig. 3. Cross section of a bifacial MIS inversion solar cell. Reprinted from Ref. [24], with the permission of WIP Renewable Energies.

With such cells open-circuit voltages of more than 650 mV and efficiencies of 19% were achieved [28,29]. The early PESC cells still had a flat front surface and thus it was a logical step to combine surface passivation with surface texturing to achieve higher efficiencies. In fact, the microgrooved PESC cell (see Fig. 4) was the first silicon solar cell to achieve efficiencies greater than 20% [30].

2.3. Front and rear surface passivation

The traditional way to improve the electrical quality of the rear surface i.e. to reduce carrier recombination was the implementation of a high-low junction commonly known as a back surface field.[1] The BSF decreases the number of minority carriers at the rear surface of the cell and thus reduces recombination rather by changing carrier statistics than reducing the surface defect density. By alloying aluminum into the rear surface of p-type silicon solar cells a robust and well-performing structure is obtained [32]. The performance can be even improved if boron is mixed into the Al paste to increase the doping concentration of the p^+-layer [33,34]. This structure has been the workhorse for the photovoltaic industry until today.

However, the potential of cells with surface passivation at front and rear is substantially higher as already shown by several groups in the 1980s. At University of New South Wales the PESC design was extended by reducing the local contacts at the rear to a minimum and passivating the rest of the rear surface with SiO_2. This cell structure featuring partial rear contacts, also well known as the PERC cell, resulted in efficiencies of more than 22% [35]. The reduced carrier recombination at the rear surface improved both the open-circuit voltage and the short-circuit current of the solar cell.[2] The current was further boosted by the increased internal reflection of light at the rear surface improving the light-trapping of weakly absorbed infrared light. In fact the system silicon-SiO_2-metal is an almost perfect mirror which benefits additionally from total reflection especially if the rear oxide is thick enough [36].

At the same time, researchers of Stanford University presented a 1-sun version [37] of an interdigitated back-contact (IBC) solar cells which was originally developed for high-concentration applications [38]. Using this sophisticated cell structure, efficiencies of 22.3% and very high open-circuit voltages above 700 mV could be achieved. As for the PERC structure, both sides of the cell are passivated very efficiently. The carrier separation takes place at the rear side at relatively small

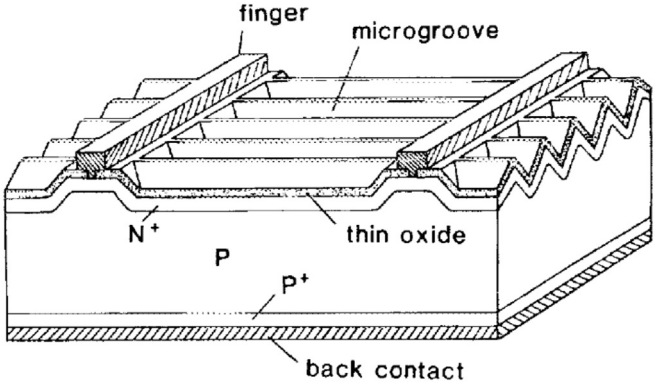

Fig. 4. Microgrooved PESC cell. Reprinted from Ref. [30], with the permission of AIP Publishing.

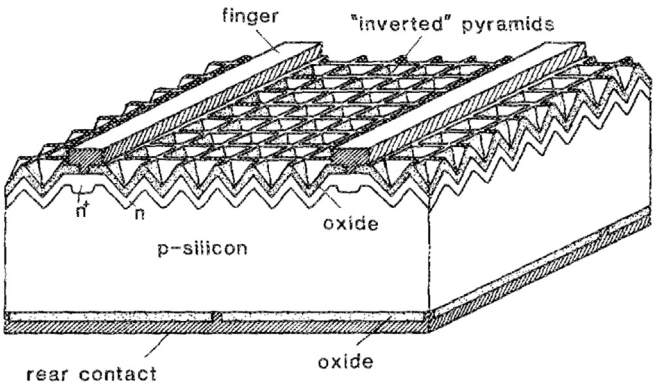

Fig. 5. Structure of a PERC cell. Reprinted from Ref. [35], with the permission of AIP Publishing.

point-like diffused regions. Thus, most of the photo-generated carriers have to diffuse from the front to the rear and the front surface passivation is of even greater importance compared to other cell architectures. A simplified version of such IBC cells [39] was the blueprint of SunPower's Gen 1 and Gen 2 IBC solar cells [40–42].

For both developments, PERC and IBC, a significantly improved oxidation using a chlorine-containing oxidation atmosphere process was used [35,43]. The addition of chlorine-containing materials like TCA or HCl to the O_2 flow during oxidation was introduced in microelectronics [14,44] since it reduces the concentration of mobile Na^+ ions which create instabilities in MOS devices. Such chlorine-containing atmosphere also removes other residual metallic impurities from the wafer surface and, therefore, considerably higher carrier lifetimes and cell efficiencies can be achieved.

In the following years both cell types reached higher and higher efficiencies finally achieving an efficiency of 25% [45,46] using the passivated emitter and rear, locally diffused cell (PERL). The main feature which was added to the original PERC cell were heavily doped p^+-regions under the rear contact points which was either achieved by boron diffusion as in the PERL structure [47,48] or aluminum alloying as in the local back surface field (Al-LBSF) structure. [49] This reduces the recombination at the remaining small metallized regions and increases the open-circuit voltage and is utilized in modern industrial cells as well. A similar feature i.e. local n^+-regions under the front contact openings also known as selective emitter was added to improve the front performance. Another improvement of the later PERL/LBSF cells was the optimization of the front side optics. Early PERC cells [35] just used a thick (~100 nm) thermal oxide at the front as passivation and antireflection layer. However, due to the low refractive index of SiO_2 this is a non-ideal solution. Therefore, thinner oxides (< 30 nm) capped by a higher refractive material like TiO_2 were used [50,51].

[1] This term is still the most commonly used term although relating the function of the high-low junction to an electric field is misleading [31].

[2] Note that the original PERC did utilize only pure ohmic rear contact points. The introduction of an additional aluminum or boron BSF was introduced later in the Local Back Surface Field (LBSF) or passivated emitter and rear, locally diffused cell (PERL) cell, respectively (see below).

However, the lower passivation quality of these thinner oxides was a challenge. Thus, an intentional *Al*neal step was introduced [52]. From microelectronics it was well known that the reduction of water in the oxide layer, which occurred at the SiO_2/Al interface at temperatures between 300 °C and 450 °C, resulted in the release of atomic hydrogen which improved the Si-SiO_2 interface significantly [53]. Such an *Al*neal step comes for free in PERC cells due to the rear Al electrode. In contrast, on the front side an additional thin Al layer was deposited, a low-temperature step was performed, the Al layer was etched and the additional antireflection layer was deposited. These front layer systems allowed for very high currents ($> 42\,mA/cm^2$) and high voltages ($> 700\,mV$). Also carrier lifetime measurements on oxide-passivated samples showed the beneficial effect of an *Al*neal step [54].

PERL cells at that time used local boron and phosphorus diffusion (as reflected by the label “locally diffused”). This process was simplified by substituting the local boron diffusion for a local laser Al firing process [55] or by thermal alloying of Al paste after an laser opening of the rear passivation layer [56]. The latter process is the standard of current industrial PRC cells with efficiencies up to 22% [12].

Due to the excellent passivation quality of SiO_2 layers, the surface recombination velocity in oxide-passivated PRC devices is strongly reduced. Additionally, the internal reflection at the Si-SiO_2-Al rear surface is very high allowing for an excellent light trapping. Therefore, it can be expected that even very thin silicon solar cells should show a very high performance. In fact, Wang et al. could fabricate a PERL cell with a thickness of 47 µm exhibiting an efficiency of 21.5% and a very high voltage of close to 700 mV [57]. Later on, it was possible to show that even on a 37 µm thin silicon solar cell it is possible to achieve an efficiency of 20.2% (V_{oc} = 675 mV, J_{sc} = 36.6 mA/cm^2, FF = 81.9%) [58,59]. Additionally, it was shown that cells on low-quality silicon benefited from the reduction of thickness due to an improved ratio of diffusion length to thickness [58].

In the last decade very attractive industrial PERC process sequences based on thermal oxidation were developed [60–62] and the production technology for thermal oxidation was improved to increase through-put [63,64]. However, due to the excellent physical properties of Al_2O_3 i.e. its strong negative built-in charge, most of today's PERC-type solar cells use Al_2O_3 with an additional SiN_x capping layer for the rear side passivation [8]. For the passivation of the front side a thin SiO_2 layer under the front SiN_x antireflection layer is still of interest, since it improves surface passivation and also reduces significantly the effect of potential-induced degradation (PID-s) [65].

3. Electrical properties of SiO_2 passivation layers

3.1. Physical properties

For the electrical characterization of dielectric passivation layers, the following physical parameters are of major interest:

- the interface state density, D_{it} (E), (unit: eV^{-1} cm^{-2}), which has to be determined as a function of energy since the defect levels are distributed over the whole bandgap,
- the capture cross sections for electrons and holes, σ_n and σ_p (unit: cm^{-2}),
- and the density of fixed charges in the layer, Q_f (unit: cm^{-2}) resulting in a shift of the flat-band voltage, V_{FB} (unit: V).

Due to the great importance of the Si-SiO_2 system for the CMOS technology it has been studied extensively in the last decades [15,66]. While capacitance voltage measurements on MOS structures are used to determine V_{FB} and D_{it} [67], a modified version of deep-level transient spectroscopy (DLTS) was used to determine σ_n and σ_p [67,68]. The main findings [69–71] are that the Si-SiO_2 interface features

- very low D_{it} values in the range of 10^{10} eV^{-1} cm^{-2} (especially after an *Al*neal step)
- capture cross sections which are highly asymmetric $\sigma_n \approx 100 \times \sigma_p$
- and a low positive fixed charge density $Q_f \approx 10^{11}$ cm^{-2} which results in a small negative V_{FB}.

3.2. Determination of surface recombination velocity

The measured values of D_{it}, Q_f, σ_n and σ_p, can be used to calculate the surface recombination velocity, S, for different doping concentrations and excess carrier densities [43,69,72,73]. The calculated S values show a decrease with decreasing doping concentrations. Due to the asymmetry of electron and hole capture cross section, S is generally lower on n-type silicon and shows a weaker dependence on the excess carrier density [43,69]. It could be shown that these predictions of the surface recombination velocity are in good agreement with values determined from quantum efficiency measurement of devices [69] and carrier lifetimes on moderately doped test samples [74]. The analysis of the SiO_2 passivation quality on highly doped silicon surfaces shows an effective surface passivation for *n*-type surfaces, i.e. phosphorus emitters [75–77]. However, the passivation quality achieved on silicon with a high boron doping was much lower [78]. In fact, high-efficiency *n*-type PERL-type cells with boron emitter showed severe instabilities [79]. Such boron emitters have to be passivated with a negatively charged dielectric layer, like Al_2O_3 [80].

Due to the rather low density of fixed oxide charge, SiO_2 fully relies on the reduction of the interface state density. This passivation mechanism is also known as chemical passivation. Other passivation layers as SiN_x or Al_2O_3 exhibit a high number of positive or negative fixed charges, respectively. This leads to a reduction of one the types of charge carrier in the underlying silicon which can reduce the surface recombination velocity, known as field-effect passivation. Such field effect passivation can be induced artificially for SiO_2 passivation layers by applying an external voltage via a gate electrode [81,82] or by deposition of corona charges [73,83,84]. In such experiments, the measured surface recombination velocity as a function of the applied charge results in a peak-shaped curve which shows very low surface recombination velocities for high positive or negative corona charge densities. A maximum recombination velocity is observed when the ratio of the hole and electron density at the interface equals the ratio of the electron and hole capture cross sections: $p_s/n_s = \sigma_n/\sigma_p$ [73]. Since the Corona surface charges are not long-term stable and can be washed away, this additional field effect passivation could not be utilized in real devices up to now. Recently, Bonilla and Wilshaw have presented a technique to create stable charges on SiO_2 based on a chemical preparation of the surface and heat treatments [85,86].

4. SiO_x for passivating contacts

As has been pointed out above, thermally grown SiO_2 layers strongly contributed to the advancement of silicon solar cell efficiency and facilitated the understanding of surface passivation schemes. While for industrial PERC/PERT cells PECVD SiN_x and PECVD (ALD) Al_2O_3 are the dominant dielectric surface passivation layers, ultra-thin SiO_x layers which are implemented into poly-Si based passivating contacts have attracted growing interest recently [87].

4.1. Metal-insulator-semiconductor junctions

An early application of ultra-thin SiO_x layers was in MIS solar cells. The insertion of a thin SiO_x layer between the c-Si substrate and the metallization led to appreciable gains in V_{oc} [88,89] compared to a Schottky contact.

The working principle of a MIS contact relies on the depletion of one type of carrier at the surface by using a metal with a suitable work function. The interfacial oxide presents a resistance to the charge carriers and reduces interface traps which would otherwise lead to an

unfavorable pinning of the Fermi level at the surface. By passivating surface states the metal-insulator barrier height φ_{mi} and the semiconductor-insulator barrier height φ_{si} determine the surface band bending in the c-Si and one obtains either a minority carrier or majority carrier diode [90]. For instance, the Al/SiO_x/c-Si(p) (φ_{mi} = 3.2 eV) structure yields an inverted c-Si surface and can function properly as a solar cell. The underlying physics regarding charge carrier transport has been subject to discussion. Apparently, the MIS theory, which describes majority carrier flow by tunneling through the oxide barrier, described most experimental observations best. This topic was thoroughly discussed in a review paper [91].

The band bending underneath the contact can be enhanced by sandwiching a 5 nm thin CsCl layer between the oxide layer and aluminum. This led to an increase in V_{oc} by about 20 mV and an efficiency of 19.6% [92]. However, a more effective approach to increase V_{oc} was the insertion of a diffused region underneath the interfacial oxide. The device was referred to as MINP solar cell and a V_{oc} of 678 mV was demonstrated on a planar solar cell [23]. After the discovery of SiN_x as a well-passivating anti-reflection coating, substantial progress in the development of the MIS-n^+p (or MINP) solar cell was attained in the Hezel group [21]. An independently confirmed efficiency of 21.1% had been reached with a textured MIS-n^+p solar cell featuring a SiO_2-based partial rear contact (PRC) scheme and a double layer ARC at the front [93] (Fig. 6).

4.2. Poly-Si based passivating contacts

4.2.1. From microelectronics to photovoltaics

Recently, interest has been renewed in poly-Si/SiO_x contacts. This technology was originally pioneered by the microelectronics industry for its application in high-speed bipolar junction transistors (BJTs) and was thoroughly reviewed by Post et al. [94]. At that time one challenge was the scaling of the base width and the lateral dimensions of these devices without increasing the peripheral component of the emitter capacitance, which would have been detrimental to its AC characteristics. This required very thin emitters which (i) were difficult to realize and (ii) suffered from increased minority carrier recombination as these emitters became transparent for minority carriers. On the other hand, the poly-Si emitter (see simplified schematic in Fig. 7b) solved both of these issues very elegantly. Firstly, the poly-Si emitter acted as a diffusion source thereby enabling the formation of a very shallow junction within the c-Si base. Secondly, minority carrier back-injection from the base into the emitter was significantly reduced. The latter effect was further strengthened by the deliberate growth of a very thin interfacial oxide before poly-Si deposition. Thereby, current gain values higher than 300 could be realized. Although the wet-chemical growth of an interfacial oxide boosted current gain, it, in turn, increased the emitter resistance significantly [94,95]. This posed a problem for BJTs where device dimensions were ever shrinking and therefore, a lot of work had been dedicated to controllably reduce the emitter resistance by applying higher thermal annealing temperatures which enhanced the break-up (or balling up) of the interfacial oxide layer but in turn diminished the current gains [96]. When applying very high annealing temperatures, the poly-Si epitaxially regrows and the structure turns into that of an extended emitter (Fig. 7c) which behaves similarly to a conventional BJT (Fig. 7d). Another distinctive structure is the SIS emitter (Fig. 7a) which refers to a poly-Si contact which is not subjected to a high-temperature anneal and, therefore, the dopants are confined to the poly-Si layer. Very high current gains of more than 10,000 were reported for this structure [97] but the current gain was a strong function of the applied voltage and, more importantly, the electrical characteristics of these devices degraded during operation [98]. Finally, the poly-Si emitter without deliberately grown interfacial oxide (still a very thin oxide is inevitably present [96]) has been commercialized as its lower emitter resistance enabled faster switching devices.

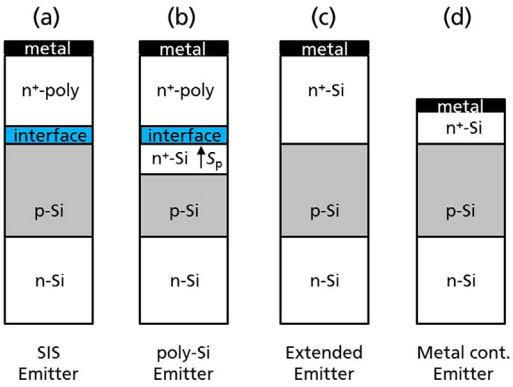

Fig. 7. Schematic diagrams of (a) an SIS emitter, (b) a polysilicon emitter, (c) an extended emitter, and (d) a metal contacted emitter (redrawn from Ref. [94]).

In contrast to BJTs, poly-Si-based contacts with interfacial oxide are the natural choice for solar cell applications as low J_0 values rather than very low contact resistivity values are required. Already in the 1980s researchers applied this technology to silicon solar cells with the aim to boost V_{oc} [26,97,99]. For instance, J_0 values of 10–20 fA/cm^2 had been obtained with poly-Si/SiO_x contacts and SIPOS (semi-insulating poly-Si) contacts [99] and a V_{oc} of 720 mV was measured on a 50 µm thin solar cell test structure where both sides were covered with n-type SIPOS and a Ga-In contact was realized at the edge [26]. For p-type poly-Si/SiO_x and SIPOS contacts significantly higher J_0 values were reported by Kwark et al. [100] which agrees with the lower gain enhancement factors of pnp transistors. Motivated by the need for very low specific contact resistivities in order to realize IBC solar cells which operate efficiently under concentrated sunlight [101], Gan and Swanson introduced poly-Si contacts with thicker, thermally grown

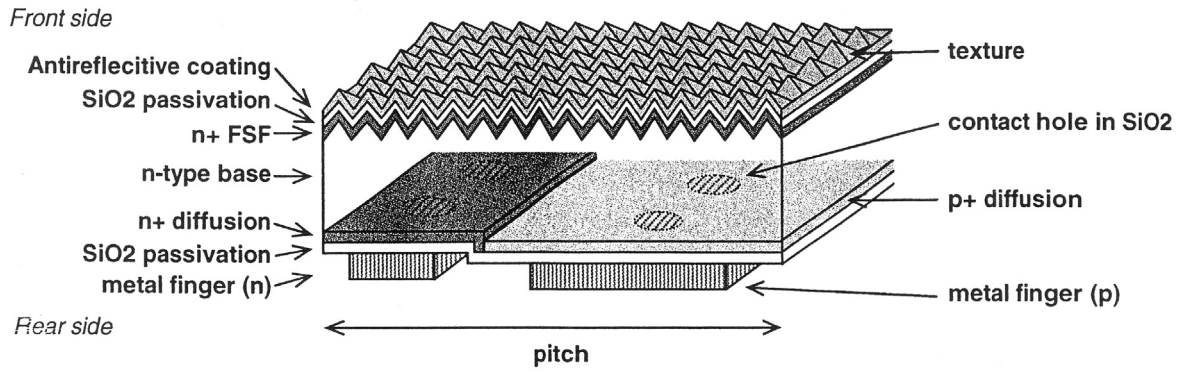

Fig. 6. IBC solar cell by SunPower. Reprinted from Ref. [40], with the permission of WIP Renewable Energies.

interfacial oxide layers which were subjected to a high-temperature anneal at 1050 °C thereby deliberately forming pinholes in the oxide layer [25]. As a result, reasonably low J_0 values of 24 fA/cm^2 (35 fA/cm^2) had been obtained at a very low specific contact resistivity of 18 μΩ cm^2 for *n*-type (*p*-type) poly-Si emitters. In the years after 1990, publications on this technology were quite rare and the next notable publication was that by Borden et al. in 2008. Their study dealt with poly-Si/SiO_x contacts realized by standard microelectronic processing equipment (RTO, LPCVD, RTP) [102]. In 2013, Feldmann et al. published the first solar cell featuring a boron-diffused emitter and a passivating rear contact (TOPCon) which achieved an efficiency of more than 23% [103,104]. Due to the one-dimensional majority carrier flow in the base of a solar cell featuring a full-area passivating contact, the excellent surface passivation, and low contact resistivity, a V_{oc} above 700 mV and FF above 82% could be achieved. The passivating contact was realized by growing a thin interfacial oxide in HNO_3, depositing a Si-rich SiC_x layer by PECVD, thermal annealing at 800–900 °C, and a hydrogen passivation step. For TOPCon structures it was shown that replacing the HNO_3 oxide for an oxide either grown in ozonated water or ozone-ambient enhanced the thermal stability (especially on textured surfaces). Furthermore, XPS measurements of the different oxides hinted at a correlation between higher stoichiometry of the oxide and better thermal stability [105].

In 2014, Römer et al. demonstrated for the first time that very low J_0 values (less than 10 fA/cm^2) can be attained with p-type poly-Si contacts [106] following the approach of Gan and Swanson. Today, several groups have reported J_0 values lower than 10 fA/cm^2 for n-type poly-Si/SiO_x passivating contacts while maintaining contact resistivities sufficiently low for solar cell contacts [104–113]. While higher J_0 values have been typically measured for p-type poly-Si/SiO_x contacts, the number of papers reporting J_0 values lower than 5 fA/cm^2 increases steadily (1 fA/cm^2 [114], 4 fA/cm^2 [115], 5 fA/cm^2 [116]). One of the key processes enabling such low J_0 values is an effective hydrogenation of the poly-Si/SiO_x contact which reduces the interface trapped charge density at the Si/SiO_x interface. Hydrogen can be effectively supplied by a hydrogen plasma (e.g. remote plasma hydrogen passivation [117]) or can be released from H-containing films like Al_2O_3 [118] or SiN_x [110,114,119]. For instance, Mack et al. reported that the J_0 of a p-type poly-Si contact was reduced from about 13 fA/cm^2 down to 1 fA/cm^2 by firing [114]. While these low J_0 values were all achieved on shiny-etched or planarized c-Si surfaces, it was reported that the J_0 of p-type contacts drastically increased on textured surfaces. By comparing planar (100)- and (111)-oriented c-Si surfaces, Larionova et al. could successfully ascribe the lower passivation quality on textured surfaces to a drastically increased recombination rate on (111) oriented surfaces [120]. The reason for this increase was attributed to the considerably higher D_{it} on (111)-oriented Si known from previous studies. Interestingly, passivating textured surfaces is not a problem for n-type poly-Si/SiO_x contacts. For instance, Stodolny *et al.* reported J_0 values as low as 4 fA/cm^2 (compared to 2 fA/cm^2 on planar surfaces) using LPCVD equipment [110]. Using industrial PECVD equipment, TOPCon structures have achieved very low J_0 values of about 2–4 fA/cm^2 and 1–2 fA/cm^2 on textured and planar surfaces, respectively [121].

Poly-Si/SiO_x passivating contacts not only enable an excellent surface passivation but also an improvement of bulk properties. It has been reported that n-type poly-Si/SiO_x contacts doped by ion implantation yielded an improved bulk lifetime [122]. Liu et al. investigated this more in detail and found a strong gettering effect for poly-Si/SiO_x contacts doped by $POCl_3$ and BBr_3 diffusion [123].

4.2.2. Charge carrier transport

For the description of charge carrier transport across the poly-Si/c-Si junction of BJTs three models were proposed: “oxide tunneling model” [125], “segregation model”, and “grain boundary mobility model”, and were compared to each other in Ref. [94]. It is important to note that the applicability of each model strongly depends on the used processes and the type of poly-Si emitter. An instructive example for BJTs can be found in Ref. [126]. It can be said that the “oxide tunneling” model explained best the reduction of the base current and the increase of the emitter resistance of BJTs with deliberately grown interfacial oxide (see Fig. 7a and b) [125]. The assumption that tunneling is the dominant transport mechanism was further substantiated by the weak temperature dependence of these devices [94,127]. The weakness of the model is that the electrical characteristics of both *npn* and *pnp* transistors cannot be explained with one unifying parameter set (with respect to electron/hole barrier height). Moreover, the model predicts that a slight current gain enhancement would come at the expense of a very high emitter resistance which does not reflect the experimental findings [128–130].

For photovoltaic applications two limiting cases of poly-Si based passivating contacts can be distinguished: (i) passivating contacts with very thin tunnel oxides [100,104] and (ii) passivating contacts with thicker oxides where tunneling is less efficient and pinholes are required for sufficiently low ρ_c values [25,106]. Both structures have in common that dopants are diffusing from the poly-Si into the c-Si during the high-temperature anneal. For type I devices the main function of this shallow diffused region is to increase the tunnel current [131] while for type II devices it reduces the recombination rate at the pinholes [132].

The impact of pinholes in the oxide on the electrical characteristics of MIS solar cells had already been discussed by Green [133]. He stated that a maximum pinhole areal density of 10^{-5} would not interfere with the electrical properties of the MIS solar cell. The effect of the high-temperature anneal on the integrity of the interfacial oxide had been studied by Wolstenholme et *al.* in great depth and the oxide break-up could be well correlated with a reduction of the emitter resistance and an increase of the base saturation current [96]. A similar trend was observed by Feldmann et al. for TOPCon structures featuring a ~1.2 nm thin oxide grown in HNO_3 (see Fig. 8). However, a reduced emitter resistance was observed for T_{anneal} = 900 °C at which the interfacial oxide seemed to be continuous according to TEM. In this state there seems to be a coexistence of tunneling and pinhole transport. By means of 2D device modelling Hamel et al. [134] could explain this result by the formation of a limited number of pinholes in the oxide which are hardly observable in TEM. Therefore, an alternative technique not only capable of visualizing pinholes but also capable of quantifying the pinhole density has been developed [135,136]. Recently, a 3D model based on a model for PERC-type solar cells [137] which accounts only for transport via pinholes was published [132,138]. The strength of this model is that it explains the symmetric behavior of n-type and p-type poly-Si contacts with thick oxides (type II) observed by Gan and

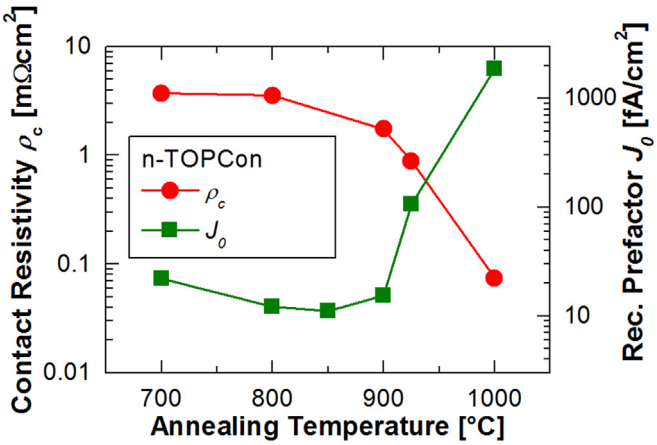

Fig. 8. J_0 and contact resistivity as a function of annealing temperature. For annealing temperatures above 900 °C the interfacial oxide loses its integrity and the recombination increases significantly [124].

Swanson [25] and Roemer et al. [106,115].

The model actually predicts two operating regimes (assuming a pinhole radius of 2 nm, see Fig. 5 in [138])

a) for very high pinhole densities above $\sim 1 \times 10^9$ cm^{-2} (corresponding to an areal density of about 10^{-4}) log(J_0) increases linearly with decreasing log(ρ_c)
b) for pinhole densities $< 1 \times 10^7$ cm^{-2} (corresponding to an areal density of about 10^{-6}) J_0 is no longer a function of the pinhole density but is dominated by the effective recombination velocity at the c-Si/SiO_x surface

Interestingly, the transition from regime a) to regime b) occurs of a pinhole areal density at around 10^{-5} as predicted by Green [133].

However, from the literature it is known that the pinhole model does not explain the *J-V* characteristics of non-annealed poly-Si/SiO_x/c-Si structures, which also yielded significant current gain enhancement factors [139]. For these devices the "oxide tunneling" model is more appropriate. Steinkemper et al. have performed a simulation study for type I passivating contact structures featuring very thin oxides considering only transport via quantum mechanical tunneling [131]. Recently, temperature-dependent *J-V* measurements of TOPCon structures featuring an about 1.2 nm thin oxide layer revealed that tunneling seems to be the dominant transport path for contacts with intact oxide [140]. This is further supported by the fact that the contact resistivity shown in Fig. 8 takes similar values for T_{anneal} = 700 °C and T_{anneal} = 800 °C. Since the formation of pinholes in the oxide is a thermally activated process described by a given activation energy, one would expect significantly different pinhole densities at 700 °C and 800 °C, respectively, and, therefore, different contact resistivities which is not the case here. Still it is conceivable that a tiny pinhole areal density exists which might help to reduce ρ_c. By applying $T_{anneal} > 900$ °C a significant density of pinholes readily forms and adversely affects the surface passivation quality provided by the passivating contact (see Fig. 8).

In conclusion, both models have their justification depending on which passivating contact structure has to be described (i.e. type I and type II). From the discussion above, it is obvious that although the principal structure of the passivating contacts is similar, the process steps differ quite significantly, particularly the thickness of the oxide and the final thermal treatment, which makes it difficult to generalize theories about the underlying physical transport mechanisms. Especially for passivating contacts with interfacial oxides thinner than 2 nm a coexistence of both current transport paths can be anticipated. The transition from type I to type II devices depends on the oxide stoichiometry and thickness as well as the applied annealing temperature.

4.2.3. Application to solar cells

The implementation of poly-Si based passivating contacts into lab-scale solar cells has enabled record efficiencies. The best solar cell featuring top/rear contacts is an n-type solar cell featuring a boron-diffused emitter and a passivating rear contact. An efficiency of 25.8% [141,142] has been demonstrated. Moreover, a world-record efficiency of 22.3% has been achieved by transferring this solar cell structure to n-type high-performance mc-Si [143]. On p-type c-Si, the first solar cell with phosphorus-doped and boron-doped TOPCon top/rear contacts achieving a V_{oc} of 694 mV and a *FF* of 81.1% was demonstrated in Ref. [144]. Nogay et al. have demonstrated that FF up to 84% can be achieved with this structure [145]. By using an IBC structure featuring both polarities at the rear an efficiency of 26.1% has been very recently reached [146].

Stodolny et al. published the first solar cell featuring a poly-Si rear contact which was processed using industrial equipment [110]. While lab cells typically feature evaporated Ag or Al contacts, contact formation was done by screen-printing Ag and fast-firing. The advantage of this process is that the SiN_x supplies hydrogen to the contact very effectively. However, it has been shown that conventional Ag pastes consumed a large fraction of the poly-Si [116]. Even for almost 300 nm thick p-type poly-Si contacts a strong increase in $J_{0,met}$ has been observed [114]. Another drawback of such thick poly-Si layers is associated with free carrier absorption which reduces the IR response of the solar cell significantly.

Considering the successful implementation of poly-Si/SiO_x passivating contacts and the very active research and development, it is likely that the next generation of industrial silicon solar cells will be based on such contact systems. This makes SiO_2 once again an important enabling technology for c-Si photovoltaics.

5. Conclusion

Due to its superior electrical properties which allow a dramatic reduction in surface recombination velocity dramatically, SiO_2 passivation layers had a strong impact on the history of silicon solar cells and allowed development of the first advanced silicon solar cell architectures such as IBC or PERC with efficiencies above 20%. Thus, it paved the way for the current rapid development in silicon photovoltaics and passivation layers as Al_2O_3 or SiN_x. Being a real evergreen, it enables technologies for the next generation of cells such as passivating contacts and is thus a true key technology for silicon photovoltaics.

Acknowledgements

The authors would like to thank sincerely all co-workers at Fraunhofer ISE who have contributed to the development of high-efficiency silicon solar cells in the last decades.

References

[1] R.M. Swanson, R.A. Sinton, High-efficiency silicon solar cells, 1st ed, in: K.W. Böer (Ed.), Advances in Solar Energy: An Annual Review of Research and Development, 6 Springer, 1990, pp. 427–484.
[2] R.J. Schwartz, Personal communication to the authors of [2], 1983.
[3] A. Richter, F. Werner, A. Cuevas, J. Schmidt, S.W. Glunz, Improved parameterization of Auger recombination in silicon, Energy Proc. 27 (2012) 88–94.
[4] A.G. Aberle, Surface passivation of crystalline silicon solar cells: a review, Prog. Photovolt.: Res. Appl. 2000 (8) (2000) 473–487.
[5] R.S. Bonilla, B. Hoex, P. Hamer, P.R. Wilshaw, Dielectric surface passivation for silicon solar cells: a review, Phys. Status Solidi (a) 25 (1–2) (2017) 1700293.
[6] A.G. Aberle, R. Hezel, Progress in low-temperature surface passivation of silicon solar cells using remote-plasma silicon nitride, Prog. Photovolt.: Res. Appl. 5 (1) (1997) 29–50.
[7] K.H. Kim, C.S. Park, J.D. Lee, J.Y. Lim, J.M. Yeon, I.H. Kim, E.J. Lee, Y.H. Cho, Record high efficiency of screen-printed silicon aluminum back surface field solar cell: 20.29%, Jpn. J. Appl. Phys. 56 (8S2) (2017) 08MB25.
[8] ITRPV, International Technology Roadmap for Photovoltaic: 2016 Results, 8th ed, 2017.
[9] B. Hoex, J. Schmidt, R. Bock, P.P. Altermatt, M.C.M. van de Sanden, W.M.M. Kessels, Excellent passivation of highly doped p-type Si surfaces by the negative-charge-dielectric Al_2O_3, Appl. Phys. Lett. 91 (11) (2007) 112107.
[10] G. Agostinelli, A. Delabie, P. Vitanov, Z. Alexieva, H.F.W. Dekkers, S. de Wolf, G. Beaucarne, Very low surface recombination velocities on p-type silicon wafers passivated with a dielectric with fixed negative charge, Sol. Energy Mater. Sol. Cells 90 (18–19) (2006) 3438–3443.
[11] P. Saint-Cast, D. Kania, M. Hofmann, J. Benick, J. Rentsch, R. Preu, Very low surface recombination velocity on p-type c-Si by high-rate plasma-deposited aluminum oxide, Appl. Phys. Lett. 95 (15) (2009) 151502.
[12] M. Müller, G. Fischer, B. Bitnar, S. Steckemetz, R. Schiepe, M. Mühlbauer, R. Köhler, P. Richter, C. Kusterer, A. Oehlke, E. Schneiderlöchner, H. Sträter, F. Wolny, M. Wagner, P. Palinginis, D.H. Neuhaus, Loss analysis of 22% efficient industrial PERC solar cells, Energy Proc. 124 (2017) 131–137.
[13] W. Deng, F. Ye, Z. Xiong, D. Chen, W. Guo, Y. Chen, Y. Yang, P.P. Altermatt, Z. Feng, P.J. Verlinden, Development of high-efficiency industrial p-type multicrystalline PERC solar cells with efficiency greater than 21%, Energy Proc. 92 (2016) 721–729.
[14] B.E. Deal, D.W. Hess, J.D. Plummer, C.P. Ho, Kinetics of the thermal oxidation of silicon in O_2/H_2O and O_2/Cl_2 mixtures, J. Electrochem. Soc. 125 (2) (1978) 339–346.
[15] E.H. Nicollian, J.R. Brews, MOS (Metal Oxide Semiconductor) Physics and Technology, Wiley-Interscience, 2002.

[16] B.E. Deal, A.S. Grove, General relationship for the thermal oxidation of silicon, J. Appl. Phys. 36 (12) (1965) 3770–3778.
[17] S.J. Fonash, Metal Thin Film Insulator Semiconductor Solar Cells, in: Proceedings of the 11th IEEE Photovoltaic Specialists Conference, Scottsdale, AZ, USA, 1975, pp. 376–380.
[18] D.L. Pulfrey, MIS solar cells: a review, IEEE Trans. Electron Devices 25 (11) (1978) 1308–1317.
[19] R.B. Godfrey, M.A. Green, 655 mV open-circuit voltage, 17.6% efficient silicon MIS solar cells, Appl. Phys. Lett. 34 (11) (1979) 790–793.
[20] M.A. Green, R.B. Godfrey, MIS solar cell—General theory and new experimental results for silicon, Appl. Phys. Lett. 29 (9) (1976) 610–612.
[21] R. Hezel, Silicon nitride for the improvement of silicon inversion layer solar cells, Solid-State Electron. 24 (9) (1981) 863–868.
[22] M.A. Green, A.W. Blakers, J. Shi, E.M. Keller, S.R. Wenham, High-efficiency silicon solar cells, IEEE Trans. Electron Devices 31 (5) (1984) 679–683.
[23] A.W. Blakers, M.A. Green, 678-mV open-circuit voltage silicon solar cells, Appl. Phys. Lett. 39 (6) (1981) 483–485.
[24] R. Hezel, W. Hoffmann, K. Jaeger, Recent Advances in Silicon Inversion Layer Solar Cells and Their Transfer to Industrial Pilot Production, in: Proceedings of the 10th EU PVSEC, Lisbon, Portugal, 1991, pp. 511–514.
[25] J.Y. Gan, R.M. Swanson, Polysilicon emitters for silicon concentrator solar cells, in: Proceedings of the 21st IEEE Photovoltaic Specialists Conference Kissimmee, Kissimmee, 1990, pp. 245–250.
[26] E. Yablonovitch, T. Gmitter, R.M. Swanson, Y.H. Kwark, A 720 mV open circuit voltage SiO_x:c-Si:SiO_x double heterostructure solar cell, Appl. Phys. Lett. 47 (11) (1985) 1211–1213.
[27] J.G. Fossum, E.L. Burgess, High-efficiency p^+ -n-n^+ back-surface-field silicon solar cells, Appl. Phys. Lett. 33 (3) (1978) 238–240.
[28] M.A. Green, A.W. Blakers, J. Shi, E.M. Keller, S.R. Wenham, 19.1% efficient silicon solar cell, Appl. Phys. Lett. 44 (12) (1984) 1163.
[29] M.A. Green, A.W. Blakers, C.R. Osterwald, Characterization of high-efficiency silicon solar cells, J. Appl. Phys. 58 (11) (1985) 4402.
[30] A.W. Blakers, M.A. Green, 20% efficiency silicon solar cells, Appl. Phys. Lett. 48 (3) (1986) 215–217.
[31] A. Cuevas, D. Yan, Misconceptions and misnomers in solar cells, IEEE J. Photovolt. 3 (2) (2013) 916–923.
[32] E.L. Ralph, Recent advancements in low cost solar cell processing, in: Proceedings of the 11th IEEE Photovoltaic Specialists Conference, Scottsdale, AZ, USA, 1975, pp. 315–316.
[33] M. Rauer, C. Schmiga, A. Raugewitz, M. Glatthaar, S.W. Glunz, Theoretical and experimental investigation of aluminum-boron codoping of silicon, Prog. Photovolt.: Res. Appl. 24 (2) (2016) 219–228.
[34] P. Lölgen, W.C. Sinke, C. Leguijt, A.W. Weeber, P.F.A. Alkemade, L.A. Verhoef, Boron doping of silicon using coalloying with aluminium, Appl. Phys. Lett. 65 (22) (1994) 2792–2794.
[35] A.W. Blakers, A. Wang, A.M. Milne, J. Zhao, M.A. Green, 22.8% efficient silicon solar cell, Appl. Phys. Lett. 55 (13) (1989) 1363–1365.
[36] D. Kray, M. Hermle, S.W. Glunz, Theory and experiments on the back side reflectance of silicon wafer solar cells, Prog. Photovolt.: Res. Appl. 16 (1) (2008) 1–15.
[37] R.R. King, R.A. Sinton, R.M. Swanson, Front and back surface fields for point-contact solar cells, in: Proceedings of the 20th IEEE Photovoltaic Specialists Conference Las Vegas, Las Vegas, USA, 1988, pp. 538–544.
[38] R.A. Sinton, Y. Kwark, J.Y. Gan, R.M. Swanson, 27.5-percent silicon concentrator solar cells, IEEE Electron Device Lett. 7 (10) (1986) 567–569.
[39] R.A. Sinton, R.M. Swanson, Simplified backside-contact solar cells, IEEE Trans. Electron Devices 37 (2) (1990) 348–352.
[40] K.R. McIntosh, M.J. Cudzinovic, D.D. Smith, W.P. Mulligan, R.M. Swanson, The choice of silicon wafer for the production of low-cost rear-contact solar cells, in: Proceedings of the 3rd World Conference on Photovoltaic Energy Conversion, Osaka, 2003, pp. 971–974.
[41] W.P. Mulligan, D.H. Rose, M.J. Cudzinovic, D.M. De Ceuster, K.R. McIntosh, D.D. Smith, R.M. Swanson, Manufacture of solar cells with 21% efficiency, in: Proceedings of the 19th European Photovoltaic Solar Energy Conference, Paris, 2004, pp. 387–390.
[42] D. de Ceuster, P. Cousins, D. Rose, D. Vicente, P. Tipones, W. Mulligan, Low cost, high volume production of > 22% efficiency silicon solar cells, in: Proceedings of the 22nd EU PVSEC, Milano, 2007, pp. 816–819.
[43] W.D. Eades, R.M. Swanson, Calculation of surface generation and recombination velocities at the Si-SiO_2 interface, J. Appl. Phys. 58 (11) (1985) 4267–4276.
[44] A. Rohatgi, S.R. Butler, F.J. Feigl, H.W. Kraner, K.W. Jones, Sodium passivation in HCl oxide films on Si, Appl. Phys. Lett. 1977 30 (1977) 104–105.
[45] M.A. Green, The path to 25% silicon solar cell efficiency: history of silicon cell evolution, Prog. Photovolt.: Res. Appl. 17 (3) (2009) 183–189.
[46] J. Zhao, A. Wang, M.A. Green, 24.5% Efficiency silicon PERT cells on MCZ substrates and 24.7% efficiency PERL cells on FZ substrates, Prog. Photovolt.: Res. Appl. 7 (6) (1999) 471–474.
[47] A. Wang, J. Zhao, M.A. Green, 24% efficient silicon solar cells, Appl. Phys. Lett. 57 (6) (1990) 602–604.
[48] J. Zhao, A. Wang, M.A. Green, 24% efficient PERL structure silicon solar cells, in: Proceedings of the 21st IEEE Photovoltaic Specialists Conference Kissimmee, Kissimmee, 1990, pp. 333–335.
[49] J. Knobloch, A.G. Aberle, B. Voss, Cost effective processes for silicon solar cells with high performance, in: Proceedings of the 9th EU PVSEC, Freiburg, 1989, pp. 777–780.
[50] S.W. Glunz, J. Knobloch, D. Biro, W. Wettling, Optimized high-efficiency silicon solar cells with J_{sc} = 42 mA/cm^2 and eta = 23.3%, in: Proceedings of the 14th European Photovoltaic Solar Energy Conference, Barcelona, 1997, pp. 392–395.
[51] J. Zhao, M.A. Green, Optimized antireflection coatings for high-efficiency silicon solar cells, IEEE Trans. Electron Devices 38 (8) (1991) 1925–1934.
[52] J. Zhao, A. Wang, P. Altermatt, S. Wenham, M. Green, 24% efficient perl silicon solar cell: recent improvements in high efficiency silicon cell research, Sol. Energy Mater. Sol. Cells 41-42 (1996) 87–99.
[53] L. Do Thanh, P. Balk, Elimination and generation of Si-SiO2 Interface traps by low temperature hydrogen annealing, J. Electrochem. Soc.: Solid-State Sci. Technol. 135 (7) (1988) 1797–1801.
[54] M.J. Kerr, A. Cuevas, Very low bulk and surface recombination in oxidized silicon wafers, Semicond. Sci. Technol. 17 (1) (2002) 35–38.
[55] E. Schneiderlöchner, R. Preu, R. Lüdemann, S.W. Glunz, Laser-fired rear contacts for crystalline silicon solar cells, Prog. Photovolt.: Res. Appl. 10 (1) (2002) 29–34.
[56] M. Rauer, R. Woehl, K. Ruhle, C. Schmiga, M. Hermle, M. Horteis, D. Biro, Aluminum alloying in local contact areas on dielectrically passivated rear surfaces of silicon solar cells, IEEE Electron Device Lett. 32 (7) (2011) 916–918.
[57] A. Wang, J. Zhao, S.R. Wenham, M.A. Green, 21.5% Efficient thin silicon solar cell, Prog. Photovolt.: Res. Appl. 4 (1) (1996) 55–58.
[58] D. Kray, H. Kampwerth, E. Schneiderlöchner, A. Grohe, F.J. Kamerewerd, A. Leimenstoll, D. Osswald, E. Schäffer, S. Seitz, S. Wassie, S.W. Glunz, G.P. Willeke, Comprehensive experimental study on the performance of very thin laser-fired high-efficiency solar cells, in: Proceedings of the 19th European Photovoltaic Solar Energy Conference, Paris, 2004, pp. 408–411.
[59] S.W. Glunz, New concepts for high-efficiency silicon solar cells, Sol. Energy Mater. Sol. Cells 90 (18–19) (2006) 3276–3284.
[60] S. Mack, A. Wolf, B. Thaidigsmann, E. Lohmüller, U. Jäger, M. Pospischil, F. Clement, D. Eberlein, R. Preu, D. Biro, Technology for mass production of > 20% efficient p-type silicon solar cells, in: Proceedings of the 28th European Photovoltaic Solar Energy Conference and Exhibition, Paris, 2013, pp. to be published.
[61] S. Mack, A. Wolf, C. Brosinsky, S. Schmeisser, A. Kimmerle, P. Saint-Cast, M. Hofmann, D. Biro, Silicon surface passivation by thin thermal Oxide/PECVD layer stack systems, IEEE J. Photovolt. 1 (2) (2011) 135–145.
[62] A. Wolf, A. Walczak, S. Mack, E. Wotke, A. Lemke, C. Bertram, U. Belledin, D. Biro, R. Preu, The SiNTO process: Utilizing a SiN_x anti-reflection layer for emitter masking during Thermal Oxidation, in: Proceedings of the 34th IEEE Photovoltaic Specialists Conference Philadelphia, Philadelphia, CA, 2009, pp. 534–539.
[63] S. Mack, A. Wolf, A. Walczak, B. Thaidigsmann, E. Allan Wotke, J.J. Spiegelman, R. Preu, D. Biro, Properties of purified direct steam grown silicon thermal oxides, Sol. Energy Mater. Sol. Cells 95 (9) (2011) 2570–2575.
[64] D. Biro, R. Preu, O. Schultz, S. Peters, D.M. Huljic, D. Zickermann, R. Schindler, R. Lüdemann, G. Willeke, Advanced diffusion system for low contamination in-line rapid thermal processing of silicon solar cells, Sol. Energy Mater. Sol. Cells 74 (1–4) (2002) 35–41.
[65] H. Nagel, P. Saint-Cast, M. Glatthaar, S.W. Glunz, Inline processes for the stabilization of p-type crystalline Si solar cells against potential-induced degradation, in: Proceedings of the 29th EU PVSEC, Amsterdam, The Netherlands, 2014, pp. 2351–2355.
[66] A. Goetzberger, E. Klausmann, M.J. Schulz, Interface states on semiconductor/insulator surfaces, Crit. Rev. Solid State Mater. Sci. (1976) 1–43.
[67] G. Barbottin, A. Vapaille, Instabilities in Silicon Devices - Silicon Passivation and Related Instabilities, Elsevier Science Publishers B.V, Amsterdam, 1986.
[68] W.D. Eades, R.M. Swanson, Improvements in the determination of interface state density using deep level transient spectroscopy, J. Appl. Phys. 56 (6) (1984) 1744–1751.
[69] A.G. Aberle, S.W. Glunz, W. Warta, Impact of illumination level and oxide parameters on Shockley–Read–Hall recombination at the Si-SiO2 interface, J. Appl. Phys. 71 (9) (1992) 4422.
[70] A.G. Aberle, S.W. Glunz, A.W. Stephens, M.A. Green, High-eficiency silicon solar cells: Si/SiO2, interface parameters and their impact on device performance, Prog. Photovolt.: Res. Appl. 2 (4) (1994) 265–273.
[71] W.D. Eades, R.M. Swanson, Determination of the capture cross section and degeneracy factor of Si-SiO_2 interface states, Appl. Phys. Lett. 44 (10) (1984) 988–990.
[72] R.B.M. Girisch, R.P. Mertens, R.F. de Keersmaecker, Determination of Si-SiO_2 interface recombination parameters using a gate-controlled point-junction diode under illumination, IEEE Trans. Electron Devices 35 (2) (1988) 203–222.
[73] S.W. Glunz, D. Biro, S. Rein, W. Warta, Field-effect passivation of the SiO_2Si interface, J. Appl. Phys. 86 (1) (1999) 683–691.
[74] S.W. Glunz, A.B. Sproul, W. Warta, W. Wettling, Injection-level-dependent recombination velocities at the Si-SiO_2 interface for various dopant concentrations, J. Appl. Phys. 75 (3) (1994) 1611–1615.
[75] R.R. King, R.A. Sinton, R.M. Swanson, Studies of diffused phosphorus emitters: saturation current, surface recombination velocity, and quantum efficiency, IEEE Trans. Electron Devices 37 (2) (1990) 365–371.
[76] S.W. Glunz, S. Sterk, R. Steeman, W. Warta, J. Knobloch, W. Wettling, Emitter dark saturation currents of high-efficiency solar cells with inverted pyramids, in: Proceedings of the 13th EU PVSEC, Nice, 1995, pp. 409–412.
[77] A. Cuevas, G. Giroult-Matlakowski, P.A. Basore, C. Dubois, R.R. King, Extraction of the surface recombination velocity of passivated phosphorus-doped silicon emitters, in: Proceedings of the 1st World Conference on Photovoltaic Energy Conversion Hawaii, Hawaii, 1994, pp. 1446–1449.
[78] R.R. King, R.M. Swanson, Studies of diffused boron emitters: saturation current, bandgap narrowing, and surface recombination velocity, IEEE Trans. Electron Devices 38 (6) (1991) 1399–1409.

[79] J. Zhao, J. Schmidt, A. Wang, G. Zhang, B.S. Richards, M.A. Green, Performance instability in n-type PERT silicon solar cells, in: Proceedings of the 3rd World Conference on Photovoltaic Energy Conversion, Osaka, 2003, pp. 923–926.
[80] J. Benick, B. Hoex, M.C.M. van de Sanden, W.M.M. Kessels, O. Schultz, S.W. Glunz, High efficiency n-type Si solar cells on Al_2O_3-passivated boron emitters, Appl. Phys. Lett. 92 (25) (2008) 253504.
[81] E. Yablonovitch, R.M. Swanson, W.D. Eades, B.R. Weinberger, Electron-hole recombination at the Si-SiO_2 interface, Appl. Phys. Lett. 48 (3) (1986) 245–247.
[82] A. Aberle, S.W. Glunz, W. Warta, Field effect passivation of high efficiency silicon solar cells, Sol. Energy Mater. Sol. Cells 29 (2) (1993) 175–182.
[83] M. Schöfthaler, R. Brendel, G. Langguth, J.H. Werner, High-quality surface passivation by corona-charged oxides for semiconductor surface characterization, in: Proceedings of the 1st World Conference on Photovoltaic Energy Conversion Hawaii, Hawaii, 1994, pp. 1509–1512.
[84] T.C. Kho, S.C. Baker-Finch, K.R. McIntosh, The study of thermal silicon dioxide electrets formed by corona discharge and rapid-thermal annealing, J. Appl. Phys. 109 (2011) 53108.
[85] R.S. Bonilla, P.R. Wilshaw, A technique for field effect surface passivation for silicon solar cells, Appl. Phys. Lett. 104 (23) (2014) 232903.
[86] R.S. Bonilla, P.R. Wilshaw, Stable field effect surface passivation of n-type Cz silicon, Energy Proc. 38 (2013) 816–822.
[87] A. Cuevas, T. Allen, J. Bullock, Y. Wan, Di Yan, X. Zhang, Skin care for healthy silicon solar cells, in: Proceedings of the 42nd IEEE Photovoltaic Specialists Conference (PVSC), New Orleans, LA, USA, 2015, pp. 1–6.
[88] S.J. Fonash, Role of interfacial layer in metal-semiconductor solar cells, J. Appl. Phys. 46 (3) (1975) 1286–1289.
[89] R.B. Godfrey, M.A. Green, 655-Mv open-circuit voltage, 17.6-percent efficient silicon mis solar-cells, Appl. Phys. Lett. 34 (11) (1979) 790–793.
[90] M.A. Green, F.D. King, J. Shewchun, Minority carrier MIS tunnel diodes and their application to electron- and photo-voltaic energy conversion—I.: theory, Solid-State Electron. 17 (6) (1974) 551–561.
[91] J. Shewchun, D. Burk, M.B. Spitzer, MIS and SIS solar cells, IEEE Trans. Electron Devices 27 (4) (1980) 705–716.
[92] C. Peters, R. Meyer, R. Hezel, MIS inversion layer silicon solar cells with 19.6% efficiency, PV in Europe. From PV Technology to Energy Solutions, 2002, 127–130.
[93] A. Metz, R. Hezel, Record efficiencies above 21% for MIS-contacted diffused junction silicon solar cells, in: Proceedings of the 26th IEEE Photovoltaic Specialists Conference Anaheim, Anaheim, USA, 1997, pp. 283–286.
[94] I.R.C. Post, P. Ashburn, G.R. Wolstenholme, Polysilicon emitters for bipolar transistors: a review and re-evaluation of theory and experiment, IEEE Trans. Electron Devices 39 (7) (1992) 1717–1731.
[95] E.F. Chor, P. Ashburn, A. Brunnschweiler, Emitter resistance of arsenic- phosphorus-doped polysilicon emitter transistors, IEEE Electron Device Lett. 6 (10) (1985).
[96] G.R. Wolstenholme, N. Jorgensen, P. Ashburn, G.R. Booker, An investigation of the thermal stability of the interfacial oxide in polycrystalline silicon emitter bipolar transistors by comparing device results with high-resolution electron microscopy observations, J. Appl. Phys. 61 (1987) 225.
[97] N.G. Tarr, A polysilicon emitter solar cell, Electron Dev. Lett. IEEE 6 (12) (1985) 655–658.
[98] H. Schaber, B. Benna, L. Treitinger, A.W. Wieder, Conduction mechanisms of polysilicon emitters with thin interfacial oxide layers, Electron Device Meeting 738–742, 1984.
[99] Y. Kwark, SIPOS heterojunction contacts to silicon, Stanford, 1984.
[100] Y. Kwark, R.A. Sinton, R.M. Swanson, Low J0 contact structures using sipos and polysilicon films, in: Proceedings of the 18th IEEE Photovoltaic Specialists Conference Las Vegas, Las Vegas, 1985, pp. 787–792.
[101] R.A. Sinton, R.M. Swanson, Design criteria for Si point-contact concentrator solar cells, IEEE Trans. Electron Devices 34 (10) (1987) 2116–2123.
[102] P. Borden, L. Xu, B. McDougall, C.P. Chang, D. Pysch, P. Voisin, S.W. Glunz, Polysilicon tunnel junctions as alternates to diffused junctions, in: Proceedings of the 23rd European Photovoltaic Solar Energy Conference and Exhibition, Valencia, 2008, pp. 1149–1152.
[103] F. Feldmann, M. Bivour, C. Reichel, M. Hermle, S.W. Glunz, A passivated rear contact for high-efficiency n-type Si solar cells enabling high Voc's and FF > 82%, in: Proceedings of the 28th European Photovoltaic Solar Energy Conference and Exhibition, Paris, 2013, pp. 988–992.
[104] F. Feldmann, M. Bivour, C. Reichel, M. Hermle, S.W. Glunz, Passivated rear contacts for high-efficiency n-type Si solar cells providing high interface passivation quality and excellent transport characteristics, Sol. Energy Mater. Sol. Cells 120 (2014) 270–274.
[105] A. Moldovan, F. Feldmann, M. Zimmer, J. Rentsch, J. Benick, M. Hermle, Tunnel oxide passivated carrier-selective contacts based on ultra-thin SiO2 layers, Sol. Energy Mater. Sol. Cells 142 (2015) 123–127.
[106] U. Römer, R. Peibst, T. Ohrdes, B. Lim, J. Krügener, E. Bugiel, T. Wietler, R. Brendel, Recombination behavior and contact resistance of n^+ and p^+ polycrystalline Si/mono-crystalline Si junctions, Sol. Energy Mater. Sol. Cells 131 (2014) 85–91.
[107] F. Feldmann, M. Simon, M. Bivour, C. Reichel, M. Hermle, S.W. Glunz, Efficient carrier-selective p- and n-contacts for Si solar cells, Sol. Energy Mater. Sol. Cells 131 (0) (2014) 100–104.
[108] D. Yan, A. Cuevas, J. Bullock, Y.M. Wan, C. Samundsett, Phosphorus-diffused polysilicon contacts for solar cells, Sol. Energy Mater. Sol. Cells 142 (2015) 75–82.
[109] M. Rienäcker, A. Merkle, U. Römer, H. Kohlenberg, J. Krügener, R. Brendel, R. Peibst, Recombination behavior of photolithography-free back junction back contact solar cells with carrier-selective polysilicon on oxide junctions for both polarities, Energy Proc. 92 (2016) 412–418.
[110] M.K. Stodolny, M. Lenes, Y. Wu, G.J.M. Janssen, I.G. Romijn, J.R.M. Luchies, L.J. Geerligs, n-Type polysilicon passivating contact for industrial bifacial n-type solar cells, Sol. Energy Mater. Sol. Cells 158 (2016) 24–28.
[111] Y. Tao, V. Upadhyaya, C.-W. Chen, A. Payne, E.L. Chang, A. Upadhyaya, A. Rohatgi, Large area tunnel oxide passivated rear contact n-type Si solar cells with 21.2% efficiency, Prog. Photovolt.: Res. Appl. 24 (6) (2016) 830–835.
[112] D.L. Young, W. Nemeth, V. LaSalvia, M.R. Page, S. Theingi, J. Aguiar, B.G. Lee, P. Stradins, Low-cost plasma immersion ion implantation doping for Interdigitated back passivated contact (IBPC) solar cells, Sol. Energy Mater. Sol. Cells 158 (2016) 68–76.
[113] F. Feldmann, C. Reichel, R. Müller, M. Hermle, The application of poly-Si/SiO_x contacts as passivated top/rear contacts in Si solar cells, Sol. Energy Mater. Sol. Cells 159 (2017) 265–271.
[114] S. Mack, J. Schube, T. Fellmeth, F. Feldmann, M. Lenes, J.-M. Luchies, Metallisation of boron-doped polysilicon layers by screen printed silver pastes, Phys. Status Solidi (RRL) - Rapid Res. Lett. 214 (2017) 1700334.
[115] U. Römer, R. Peibst, T. Ohrdes, B. Lim, J. Krugener, T. Wietler, R. Brendel, Ion implantation for poly-si passivated back-junction back-contacted solar cells, IEEE J. Photovolt. 5 (2) (2015) 507–514.
[116] H.E. Çiftpınar, M.K. Stodolny, Y. Wu, G.J.M. Janssen, J. Löffler, J. Schmitz, M. Lenes, J.-M. Luchies, L.J. Geerligs, Study of screen printed metallization for polysilicon based passivating contacts, Energy Proc. 124 (2017) 851–861.
[117] S. Lindekugel, H. Lautenschlager, T. Ruof, S. Reber, Plasma hydrogen passivation for crystalline silicon thin-films, in: Proceedings of the 23rd European Photovoltaic Solar Energy Conference and Exhibition, Valencia, 2008, pp. 2232–2235.
[118] B. Nemeth, D.L. Young, M.R. Page, V. LaSalvia, S. Johnston, R. Reedy, P. Stradins, Polycrystalline silicon passivated tunneling contacts for high efficiency silicon solar cells, J. Mater. Res. 31 (06) (2016) 671–681.
[119] G. Nogay, J. Stuckelberger, P. Wyss, E. Rucavado, C. Allebe, T. Koida, M. Morales-Masis, M. Despeisse, F.J. Haug, P. Loper, C. Ballif, Interplay of annealing temperature and doping in hole selective rear contacts based on silicon-rich silicon-carbide thin films, Sol. Energy Mater. Sol. Cells 173 (2017) 18–24.
[120] Y. Larionova, M. Turcu, S. Reiter, R. Brendel, D. Tetzlaff, J. Krugener, T. Wietler, U. Hohne, J.D. Kahler, R. Peibst, On the recombination behavior of p(+)-type polysilicon on oxide junctions deposited by different methods on textured and planar surfaces, Phys. Status Solidi a-Appl. Mater. Sci. 214 (8) (2017).
[121] B. Steinhauser, J.-I. Polzin, F. Feldmann, M. Hermle, S.W. Glunz, submitted to, Solar RRL, 2018. Solar RRL, DOI: 10.1002/solr.201800068.
[122] J. Krugener, F. Haase, M. Rienacker, R. Brendel, H.J. Osten, R. Peibst, Improvement of the SRH bulk lifetime upon formation of n-type POLO junctions for 25% efficient Si solar cells, Sol. Energy Mater. Sol. Cells 173 (2017) 85–91.
[123] A. Liu, Di Yan, S.P. Phang, A. Cuevas, D. Macdonald, Effective impurity gettering by phosphorus- and boron-diffused polysilicon passivating contacts for silicon solar cells, Sol. Energy Mater. Sol. Cells (2017).
[124] F. Feldmann, Carrier-selective contacts for high-efficiency Si solar cells, Dissertation, Freiburg im Breisgau, 2015.
[125] H.C. de Graaff, J.G. de Groot, The SIS tunnel emitter: a theory for emitters with thin interface layers, Electron Dev. IEEE Trans. 26 (11) (1979) 1771–1776.
[126] B. Soerowirdjo, P. Ashburn, Effects of surface treatments on the electrical characteristics of bipolar-transistors with polysilicon emitters, Solid-State Electron. 26 (5) (1983) 495–498.
[127] P. Ashburn, B. Soerowirdjo, Comparison of experimental and theoretical results on polysilicon emitter bipolar-transistors, IEEE Trans. Electron Devices 31 (7) (1984) 853–860.
[128] C.M. Maritan, N.G. Tarr, Polysilicon emitter P-N-P transistors, IEEE Trans. Electron Devices 36 (6) (1989) 1139–1144.
[129] A.P. Laser, K.M. Chu, D.L. Pulfrey, C.M. Maritan, N.G. Tarr, An investigation of Pnp polysilicon emitter transistors, Solid-State Electron. 33 (7) (1990) 813–818.
[130] I.R.C. Post, P. Ashburn, Investigation of boron-diffusion in polysilicon and its application to the design of P-N-P polysilicon emitter bipolar-transistors with shallow emitter junctions, IEEE Trans. Electron Devices 38 (11) (1991) 2442–2451.
[131] H. Steinkemper, F. Feldmann, M. Bivour, M. Hermle, Numerical simulation of carrier-selective electron contacts featuring tunnel oxides, IEEE J. Photovolt. 5 (5) (2015) 1348–1356.
[132] R. Peibst, U. Roemer, K.R. Hofmann, B. Lim, T.F. Wietler, J. Kruegener, N.P. Harder, R. Brendel, A simple model describing the symmetric i-v characteristics of p polycrystalline Si/n monocrystalline Si, and n polycrystalline Si/p monocrystalline Si junctions, Photovolt. IEEE J. 4 (3) (2014) 841–850.
[133] M.A. Green, Effects of pinholes, oxide traps, and surface-states on mis solar-cells, Appl. Phys. Lett. 33 (2) (1978) 178–180.
[134] J.S. Hamel, D.J. Roulston, C.R. Selvakumar, G.R. Booker, 2-Dimensional analysis of emitter resistance in the presence of interfacial oxide breakup in polysilicon emitter bipolar-transistors, IEEE Trans. Electron Dev. 39 (1992) 2139–2146.
[135] D. Tetzlaff, J. Krugener, Y. Larionova, S. Reiter, M. Turcu, F. Haase, R. Brendel, R. Peibst, U. Hohne, J.D. Kahler, T.F. Wietler, A simple method for pinhole detection in carrier selective POLO-junctions for high efficiency silicon solar cells, Sol. Energy Mater. Sol. Cells 173 (2017) 106–110.
[136] T.F. Wietler, D. Tetzlaff, J. Krügener, M. Rienäcker, F. Haase, Y. Larionova, R. Brendel, R. Peibst, Pinhole density and contact resistivity of carrier selective junctions with polycrystalline silicon on oxide, Appl. Phys. Lett. 110 (25) (2017) 253902.
[137] B. Fischer, Loss analysis of crystalline solar cells using photoconductance and

quantum efficiency Measurements, Ph.D. Thesis, Konstanz, 2003.
[138] R. Peibst, U. Römer, Y. Larionova, M. Rienäcker, A. Merkle, N. Folchert, S. Reiter, M. Turcu, B. Min, J. Krügener, D. Tetzlaff, E. Bugiel, T. Wietler, R. Brendel, Working principle of carrier selective poly-Si/c-Si junctions: is tunnelling the whole story? Sol. Energy Mater. Sol. Cells 158 (158) (2016) 60–67.
[139] M.B. Rowlandson, N.G. Tarr, A true polysilicon emitter transistor, IEEE Electron Dev. Lett. 6 (6) (1985) 288–290.
[140] F. Feldmann, G. Nogay, P. Löper, D.L. Young, B.G. Lee, P. Stradins, M. Hermle, S.W. Glunz, Charge carrier transport mechanisms of passivating contacts studied by temperature-dependent J-V measurements, Sol. Energy Mater. Sol. Cells 178 (2018) 15–19.
[141] A. Richter, J. Benick, F. Feldmann, A. Fell, M. Hermle, S.W. Glunz, n-Type Si solar cells with passivating electron contact: identifying sources for efficiency limitations by wafer thickness and resistivity variation, Sol. Energy Mater. Sol. Cells 173 (2017) 96–105.
[142] M.A. Green, Y. Hishikawa, E.D. Dunlop, D.H. Levi, J. Hohl-Ebinger, A.W.Y. Ho-Baillie, Solar cell efficiency tables (version 51), Prog. Photovolt.: Res. Appl. 26 (1) (2018) 3–12.
[143] J. Benick, A. Richter, R. Muller, H. Hauser, F. Feldmann, P. Krenckel, S. Riepe, F. Schindler, M.C. Schubert, M. Hermle, A.W. Bett, S.W. Glunz, High-efficiency n-Type HP mc silicon solar cells, IEEE J. Photovolt. 7 (5) (2017) 1171–1175.
[144] F. Feldmann, M. Simon, M. Bivour, C. Reichel, M. Hermle, S.W. Glunz, Carrier-selective contacts for Si solar cells, Appl. Phys. Lett. 104 (18) (2014).
[145] G. Nogay, in: Proceedings of the 33rd EU PVSEC, Amsterdam, The Netherlands, 2017.
[146] F. Haase, presented at SiliconPV, 2018.